ARCHIVIO ISTITUZIONALE
DELLA RICERCA

Alma Mater Studiorum Università di Bologna
Archivio istituzionale della ricerca

Playing supramolecular dominoes with light: Building and breaking a photoreversible G-quadruplex made from guanosine, boric acid and an azobenzene

This is the final peer-reviewed author's accepted manuscript (postprint) of the following publication:

Published Version:
Playing supramolecular dominoes with light: Building and breaking a photoreversible G-quadruplex made from guanosine, boric acid and an azobenzene / Pieraccini S.; Campitiello M.; Carducci F.; Davis J.T.; Mariani P.; Masiero S.. - In: ORGANIC & BIOMOLECULAR CHEMISTRY. - ISSN 1477-0520. - STAMPA. - 17:10(2019), pp. 2759-2769. [10.1039/c9ob00193j]

Availability:
This version is available at: https://hdl.handle.net/11585/691222 since: 2020-02-27

Published:

DOI: http://doi.org/10.1039/c9ob00193j

Terms of use:

Some rights reserved. The terms and conditions for the reuse of this version of the manuscript are specified in the publishing policy. For all terms of use and more information see the publisher's website.

This item was downloaded from IRIS Università di Bologna (https://cris.unibo.it/).
When citing, please refer to the published version.

(Article begins on next page)

09 April 2024

This is the final peer-reviewed accepted manuscript of:

Playing supramolecular dominoes with light: building and breaking a photoreversible G-quadruplex made from guanosine, boric acid and an azobenzene. S. Pieraccini, M. Campitiello, F. Carducci, J. T. Davis, P. Mariani, S. Masiero, Org. Biomol. Chem., 2019,17, 2759-2769

The final published version is available online at: http://dx.doi.org/10.1039/c9ob00193j

Rights / License:

The terms and conditions for the reuse of this version of the manuscript are specified in the publishing policy. For all terms of use and more information see the publisher's website.

This item was downloaded from IRIS Università di Bologna (https://cris.unibo.it/)

When citing, please refer to the published version.

Playing supramolecular dominoes with light: building and breaking a photoreversible G-quadruplex made from guanosine, boric acid and an azobenzene†

Silvia Pieraccini,[a] Marilena Campitiello,[a] Federica Carducci,[b] Jeffery T. Davis,[*c] Paolo Mariani*[b] and Stefano Masiero[*a]

Addition of azobenzene-derivative **1** in its *E* configuration to an aqueous solution containing various guanosine borate esters induces a helical G-quartet based self-organization, stabilized by intercalation of the dye. The process is driven, in a domino fashion, by the initial host–guest interaction between the dye and a specific guanosine borate diester, whose structure can be thus assigned. This inclusion complex templates the formation of G-quartets. The quartets, in turn, pile up to form a supramolecular G-quadruplex structure, in which other G species present in solution are progressively included. The G-quadruplex can be reversibly broken and reformed by photoisomerization of the dye. This hierarchical and photosensitive self-assembly is unprecedented for simple guanosine derivatives.

Introduction

Photocontrol of self-assembly offers the intriguing possibility of cycling a system between different aggregation states without the need for chemicals,[1] whose addition can cause an incremental loss of system purity and performance. For this reason, photoresponsive units have been introduced in a wide range of systems, ranging from polymers to liquid crystals, nanoparticles and molecular motors.[2] Photoswitchable units have also been introduced into biomolecular systems to control self-assembly processes. Photocontrolled DNA assembly,[3] and in particular formation of guanosine (G) quartets (G4),[4] has been reported by several groups. In some cases,[5] the photoactive moiety was covalently bound to G. In other examples, the photoactive unit was an independent component, which self-assembled onto a pre-formed G4 assembly.[6] Guanosine, which is relatively insoluble in water, can react with boric acid in the presence of KOH (or LiOH) to form a mixture (GBK or GBLi, respectively) containing equal amounts of two diastereomeric borate diesters **GBG-1** and **GBG-2**, a borate monoester **GB** and unreacted guanosine $\mathbf{G_{unr}}$ (Chart 1). Above the critical concentration of about 15 mM (as total G), a soluble GBK mixture, for instance, can give rise to hydrogels whose matrix is based on supramolecular assemblies composed of stacked G4·K^+ quartets.[7]

During our attempts to obtain a G4-based hydrogel that would be photoresponsive, we tested – among others – the azobenzene dye **1** (Chart 1). This dye has been reported by Zhou to be able to induce G-quadruplex DNA formation.[6] While **1** turned out to be ineffective in promoting sol–gel photoconversion of the guanosine-borate hydrogels, we were surprised to find that addition of ***E*-1** destabilized a preformed GBK gel: for instance, a 25–30 mM GBK mixture forms a self-standing gel, but addition of ***E*-1** transformed that stable gel into a sol (see Picture S1 in ESI†). According to the above-mentioned literature on the interaction of ***E*-1** with G-quadruplex DNA,[6] we had expected a stabilization of the gel supramolecular structure by the added dye. We therefore investigated the GBK/**1** system at concentrations ranging from solution to gel, and this led us to discover that, in solution, photoisomerization of **1** enables a light-driven, hierarchical and reversible self-assembly process. As summarized in Fig. 1, addition of ***E*-1** to the GBK solution induces the formation of G-quadruplexes (**Q1** and/or **Q2**, depending on the amount of added dye). Importantly, photoirradiation of that GBK solution containing G-quadruplexes **Q1** and/or **Q2** results in isomerization of the diazo dye to ***Z*-1**, with concomitant disassembly of **Q1** and/or **Q2** to give the monomeric components of the GBK solution (**GBG-1**, **GBG-2**, **GB** and $\mathbf{G_{unr}}$) Our data indicate a key role for one of the 2 diaster-

[a]*Dipartimento di Chimica "Giacomo Ciamician", Università di Bologna, v. S. Giacomo, 11-40126 Bologna, Italy. E-mail: stefano.masiero@unibo.it*

[b]*Dipartimento di Scienze della Vita e dell'Ambiente, Università Politecnica delle Marche, Via Brecce Bianche, 60131 Ancona, Italy. E-mail: p.mariani@staff.univpm.it*

[c]*Dept. of Chemistry and Biochemistry, University of Maryland, College Park, MD 20742, USA. E-mail: jdavis@umd.edu*

†Electronic supplementary information (ESI) available. See DOI: 10.1039/c9ob00193j

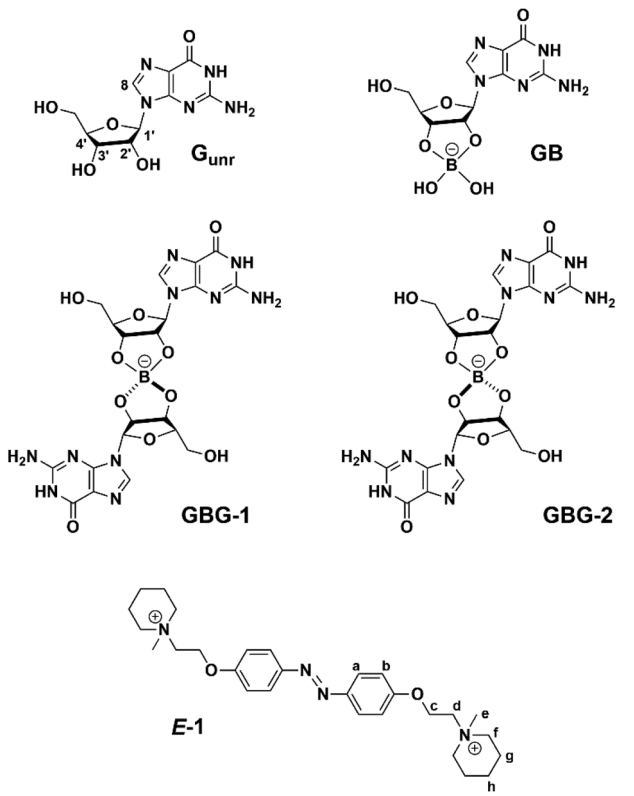

Chart 1 Structures of the molecular components that make up the GBK mixture in solution and structure of the azo dye ***E*-1** used in this study.

eomeric borate diesters, namely the C-shaped **GBG-1**, which has a cleft that allows for binding of ***E*-1**. Formation of **Q1** or **Q2**, **species that we can identify by ^{1}H NMR, CD spectroscopy or SAXS**, is likely to involve the supramolecular complexes **Ic** and **Oc** as **transient intermediates**. Indeed, we could not isolate the putative complexes **Ic** and **Oc** as stable species. We emphasize that the process illustrated in Fig. 1 is not a stepwise process, but rather it is likely to be a complex cascade of equilibria among various molecular and supramolecular species. This photoswitchable formation and disassembly of G4 supramolecular structures, made simply by mixing guanosine itself, $KB(OH)_4$ and azo-dye **1** in water, is unprecedented for low-molecular weight guanosine derivatives. On the other hand, the dye has a disruptive effect on the GBK gel matrix, for reasons that will be discussed below.

Results and discussion

NMR investigations

^{1}H-NMR spectra of ***E*-1** and GBK mixture are reported in Fig. 2a and b, respectively. The signals of the four species are assigned by comparison with spectra of pure **G**, pure **GB** (see below) and *via* COSY and NOESY correlations. From signal integration (H1′, H2′ or H3′ in Fig. 2b), in a 10 mM GBK mixture (here and throughout the text GBK concentration is meant as total G concentration) the concentration of both **GBG-1** and **GBG-2** is *ca.* 0.75 mM, borate monoester **GB** is 2 mM and unreacted guanosine $\mathbf{G_{unr}}$ is 5 mM. Thus, **GBG-1** and **GBG-2** account each for 15% of total G, **GB** accounts for 20% and $\mathbf{G_{unr}}$ accounts for 50%. Addition of ***E*-1** to GBK (*ca.* 1 : 3 molar ratio, based on total G concentration) results in the appearance of a set of broad signals (marked with rhombuses, Fig. 2c), which we ascribe to a new aggregated G-species (*bound-Gs*, **Q2** in Fig. 1), while residual sharp peaks corres-

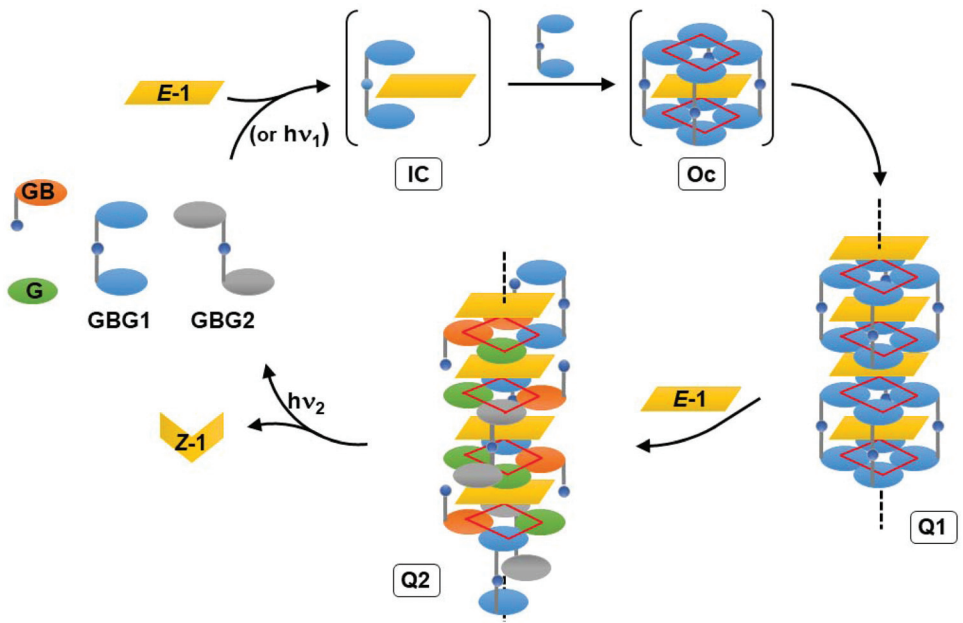

Fig. 1 Cartoon of the domino GBK/**1** self-assembly/disassembly in solution photoswitchable process that responds to the photoisomerization of azo-**1**. For sake of clarity, ribbon structures are not considered (see below).

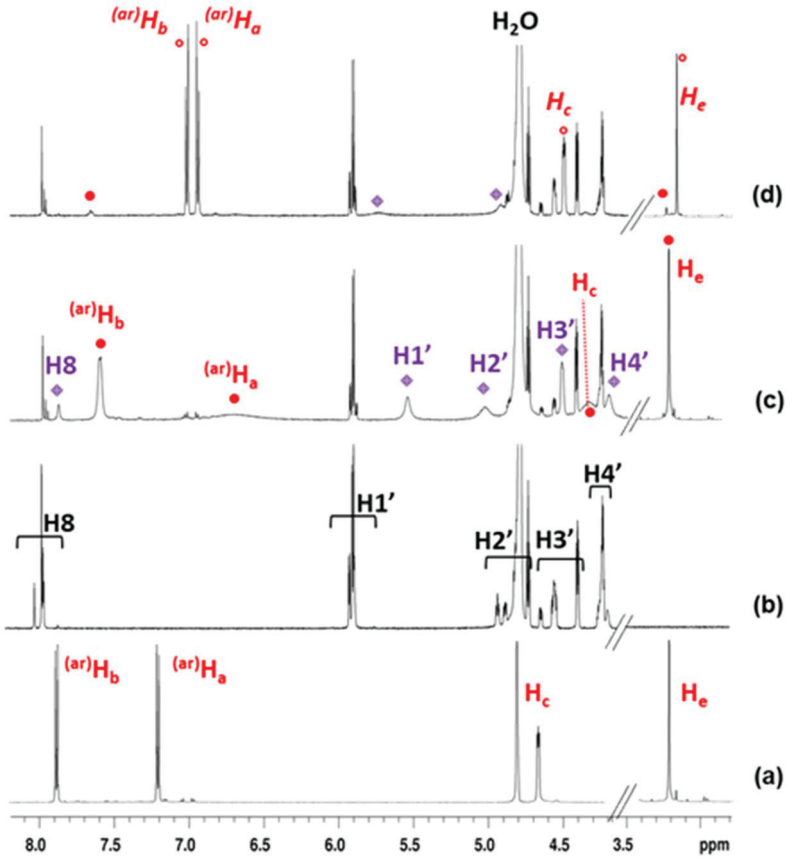

Fig. 2 ^{1}H NMR spectra recorded in D_2O at 25 °C on (a) 3 mM solution of ***E*-1**, (b) 10 mM GBK solution, (c) 10 mM GBK solution in the presence of ***E*-1** 3 mM ([total-G]/[***E*-1**] = 3). Spectrum (d) is obtained after irradiating sample (c) at 365 nm for 5 h. Proton signals corresponding to associated guanosines (purple rhombuses), ***E*-1** (full red circles) and ***Z*-1** (empty red circles) are indicated.

ponding to uncomplexed guanosines (*free-Gs*) are still present. In these conditions, the associated guanosines represent 52% of the total, as determined by the relative intensities of integrals corresponding to H1′ of *free-* and *bound-Gs*. At the same time, the NMR signals for the dye, particularly the aromatic signals, become significantly broadened and upfield-shifted, suggesting an intermolecular interaction between the dye and the newly assembled G-species. Irradiation of the GBK/***E*-1** solution at 365 nm results in disassembly of the supramolecular dye-G complex. Fig. 2d shows the spectrum recorded after 5 h of irradiation: from the integration of H′$_1$ signals we determined that 20% of the total G species are still bound to dye **1**, while the diastereomeric ratio for **1** is $Z:E$ 85 : 15, as determined from integration of the dye's He proton signals. Indeed, as we discuss below (see Fig. 5 and related discussion), when ***Z*-1** : ***E*-1** = 85 : 15, the [total-G]/[***E*-1**] molar ratio in solution is 20 : 1, and 20% of the total guanosine species in solution are expected to complex the dye ***E*-1**, consistent with the 4 : 1 stoichiometry for the G-quadruplexes **Q1** and **Q2** shown in Fig. 1.

As shown in Fig. 2d, the broad ^{1}H NMR signals for the G complex (compare with Fig. 2c) disappear almost completely upon photoisomerization. At the same time, sharp signals attributable to both *free-Gs* and the ***Z*-1** dye appear. The supramolecular dye-G complex can be reformed by irradiating this solution with 436 nm light. Indeed, under these conditions all the broad peaks of the complex increase again at the expenses of the *free-G* signals and a ^{1}H NMR spectrum like the one shown in Fig. 2c is regained. Variable temperature NMR experiments demonstrate that the G/***E*-1** aggregate is easily and reversibly broken thermally. On heating the sample from 25 °C to 75 °C (Fig. S1 in ESI†), the peaks corresponding to complexed Gs (*bound-Gs*) progressively vanish and, like the signals for ***E*-1**, become sharper and move downfield. At 75 °C, the NMR data show that both GBK and ***E*-1** are in their monomeric forms. The initial ^{1}H NMR spectrum for the G/***E*-1** aggregate, with its characteristic broad signals, can be fully recovered by cooling the sample back to 25 °C.

NOESY spectra (Fig. 3, Fig. S2 and S3†) show in-phase cross-peaks for the G/***E*-1** complex, as expected for high molecular weight aggregates. A clear intramolecular interaction is detected between H8 and H2′ protons of the *bound-Gs* at 7.85 and 5.01 ppm, respectively, while no H8–H1′ contact is seen by both 2D and 1D NOESY spectra. These NOESY data are consistent with an exclusive *anti* conformation around the glycosidic bond for Gs involved in the G/***E*-1** complex. On the contrary, *free-Gs* show anti-phase NOE cross-peaks for H8 with both H1′

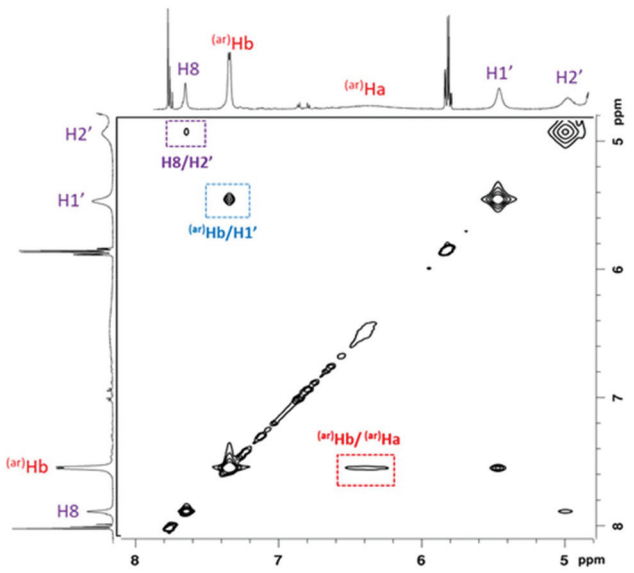

Fig. 3 2D NOESY spectrum recorded in D_2O at 25 °C on the sample containing 10 mM GBK solution in the presence of ***E*-1** 3 mM ([total-G]/[***E*-1**] = 3). Proton signals and cross-peaks corresponding to associated guanosines and ***E*-1** are indicated in purple and red, respectively. The intermolecular NOE cross-peak arising from the "associated" G/dye interaction is shown in blue.

and H2′ in 1D experiments (data not shown), indicating that both the *anti* and *syn* conformers are populated in the non-aggregated species.

The NOE data in Fig. 3 also reveals a dipolar interaction between dye molecules and the self-associated Gs. Indeed, a strong intermolecular NOE is observed between the Hb aromatic protons of ***E*-1** and the H1′ sugar proton of the *bound-Gs*. In addition, by cooling the sample to 10 °C the broadened aromatic Ha protons of the dye emerge from the baseline at *ca.* 5.8 ppm, and show a strong NOE contact with H1′ of aggregate Gs (data not shown). According to DOSY experiments, both the *bound-Gs* and ***E*-1** dye have the same diffusion coefficient (D = 2.07 ± 0.04 × 10^{-10} m^2 s^{-1}), and they also diffuse more slowly than the uncomplexed G species (*e.g.*, D_{GB} = 4.57 ± 0.11 × 10^{-10} m^2 s^{-1}). The ability of the ***E*-1** dye to template the assembly of *free-Gs* in solution is evidenced by a series of NMR titration experiments (Fig. 4). Spectra show that upon increasing the amount of dye, signals for *bound-Gs* progressively move upfield and their relative intensities increase at the expense of signals for *free-Gs* in solution. In particular, the titration data show that when the [total-G]/[***E*-1**] is >6, aggregation increases almost linearly with the amount of added ***E*-1** dye, ultimately giving a [*bound-Gs*]/[***E*-1**] molar ratio of 4 (see Fig. 5). This 4 : 1 stoichiometry is consistent with a G4 species being the structural motif that gives rise to the G-aggregates in

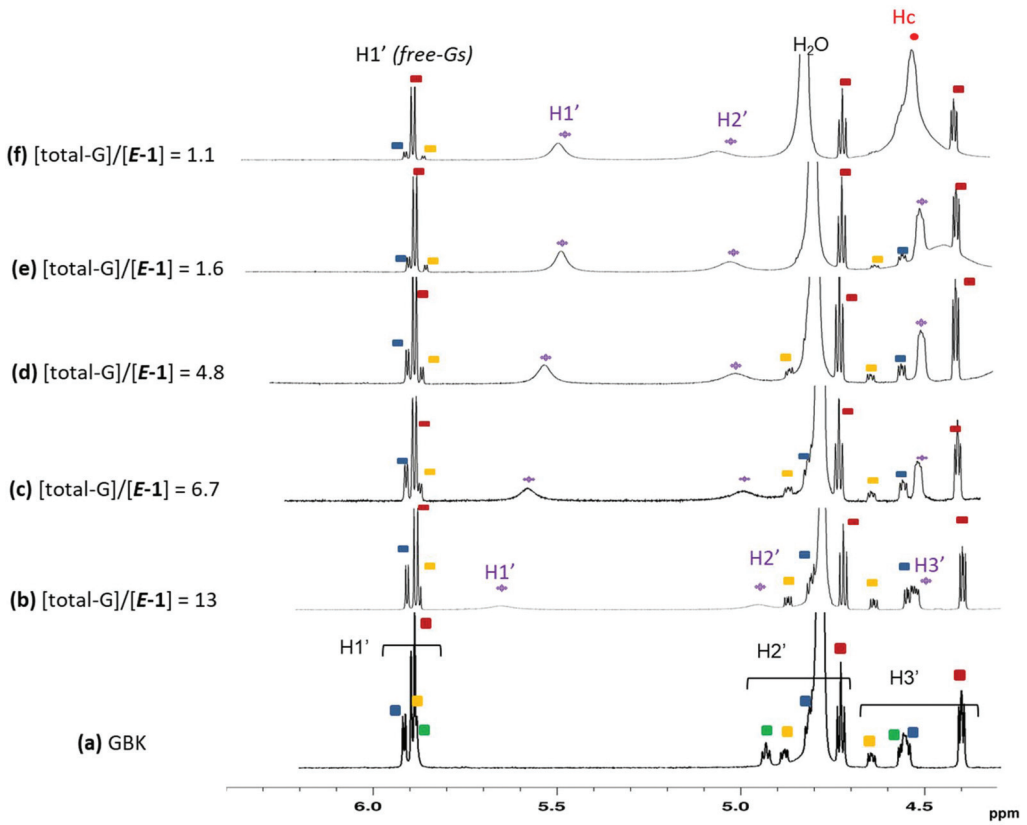

Fig. 4 ^{1}H NMR spectra recorded in D_2O at 25 °C on the 10 mM GBK solution before (a) and after addition of increasing amounts of ***E*-1** (b–f). Protons of the free G-analogues are labelled with green (**GBG-1**), yellow (**GBG-2**), blue (**GB**) and dark red squares (G_{unr}). Proton signals corresponding to associated guanosines are marked with purple rhombuses, those corresponding to ***E*-1** with full red circles.

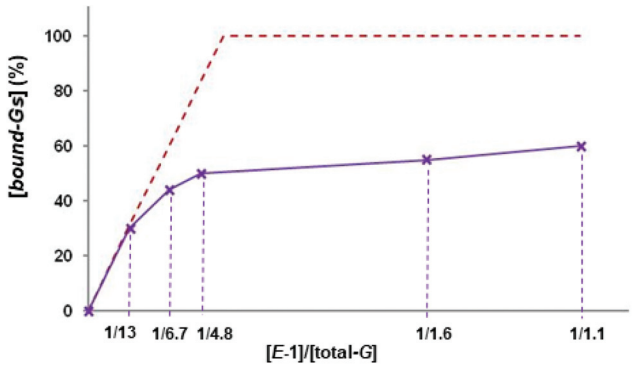

Fig. 5 Percentage of associated guanosines plotted against the [***E*-1**]/[total-G] molar ratio. Purple trace: Percentages of *bound-Gs* experimentally obtained for different dye concentrations. Data refer to ^{1}H NMR spectra shown in Fig. 4: signals from H_e of the dye and H1′ or H4′ of Gs are used for integration to obtain the [***E*-1**]/[total-G] molar ratios; the percentage of *bound-Gs* (and *free-Gs*) are calculated from the relative intensities of corresponding H1′ signals. DMSO is used as an internal standard. Red trace: Percentages of *bound-Gs* theoretically expected for the different dye concentrations, by assuming that all guanosines of the 10 mM GBK solution can participate in the G/***E*-1** complexation, on the basis of a [G] : [***E*-1**] stoichiometry of 4 : 1. These percentages are calculated as 100 × 4 × [***E*-1**]/[G].

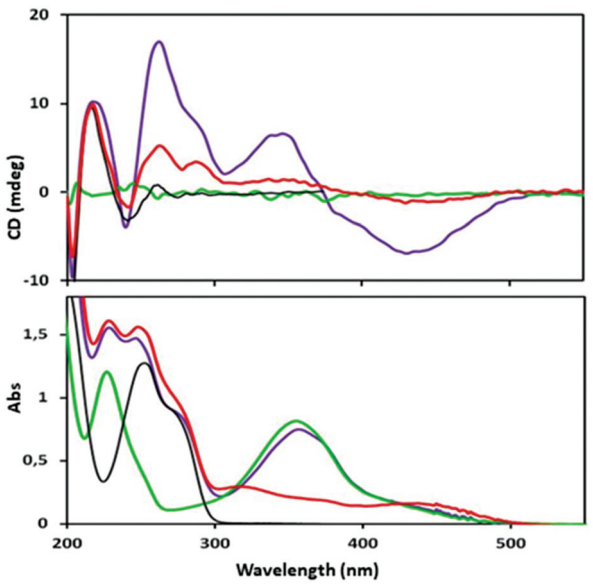

Fig. 6 CD/UV spectra recorded in H_2O at room temperature on a 10 mM solution of GBK in the absence (black line) and in the presence of ***E*-1** 3 mM ([total-G]/[***E*-1**] = 3, purple line). The *cis*-photostationary state (red line) is reached by irradiating the GBK/***E*-1** sample at 365 nm for 10 min. The trace corresponding to a 3 mM aqueous solution of ***E*-1** is reported for comparison (green line).

solution (namely **Q1** and **Q2** in Fig. 1). Further additions of dye (*i.e.*, when [total-G]/[**1**] becomes ≤6) induces progressively less aggregation and the aggregation process is complete when *bound-Gs* reach *ca.* 60% of the total G species in solution.

As determined from the relative intensities of NMR signals corresponding to the various G species, before and after addition of the dye ***E*-1**, all 4 compounds ($\mathbf{G_{unr}}$, **GB**, **GBG-1** and **GBG-2**) are involved in the formation of the G4-based aggregate. Nonetheless, signals ascribed to the diester **GBG-1** are both the first and the only ones that completely disappear upon addition of the ***E*-1** dye (for example, compare spectra (a) and (b) in Fig. 4). Overall, the NMR data point to the concentration of the diastereoisomer **GBG-1** as being the limiting factor for dye-induced aggregation. In fact, in the initial GBK solution **GBG-1** contributes to the total G concentration by *ca.* 15%. Assuming that the final structure of the aggregated species (**Q2**) has at least one unit of **GBG-1** per G4 layer (see below), the maximum amount of *bound-Gs* that form the 4 : 1 [*bound-Gs*]/[***E*-1**] complex should be 60% of the total Gs, which is in accordance with the observed experimental value determined by ^{1}H NMR. All these observations point toward a key role for borate diester **GBG-1** as the essential building block, acting in concert with the dye ***E*-1**, to template formation of this G4-based assembly.

CD analysis

A further insight into the nature of the GBK/***E*-1** complex and its photochemical behaviour is provided by CD investigation. The room temperature spectrum of a 10 mM GBK solution (Fig. 6) shows a weak signal in the 200–300 nm absorption region of guanine, suggesting that, at this low concentration, the G species are monomeric or might be organized into H-bonded ribbon-like oligomers[8] (compare SAXS data discussed below) inspite of the presence of 0.5 eq. (with respect to G) of potassium ions. Importantly, the CD spectrum changes significantly when the templating dye is added. Thus, when ***E*-1** is added to GBK (*ca.* 1 : 3 molar ratio of dye to total Gs) the resulting CD spectrum shows a positive band at 280 nm, and an intense (positive and non-conservative) exciton coupling centered at 260 nm, as is typically observed for structures that are made by helical stacking of G4 units. In addition to this signature band for the helical G-quartets, intense CD signals emerge in the 300–550 nm absorption region for the achiral azo dye. In particular, a negative induced CD signal arises at 450 nm, which corresponds to the n–π* electronic transition, while a negative exciton coupling appears at *ca.* 360 nm, corresponding to the π–π* transition for the azo-chromophore in ***E*-1**. This high optical activity confirms the strong interaction between ***E*-1** and the chiral G supramolecular assembly, as previously determined from the NMR analysis. Most remarkably, the exciton nature of the 360 nm signal suggests a helical arrangement of close-in-space azo-moieties, possibly intercalating between adjacent G-quartets. Note that the 260 nm centered exciton originates only from guanine chromophore. An induced CD originating from phenyl chromophores of the azo dye should appear at lower wavelengths (226 nm, see UV green spectrum in Fig. 6), either as a monosigned band or as a couplet centered at 226 nm. In either case, the CD spectrum around this wavelength should differ from the pure GBK sample. The existence

of a significant ICD arising from the phenyl chromophore can thus be ruled out by comparing the CD spectra of GBK in the presence (purple and red spectra in Fig. 6) and in the absence of dye (black spectrum in Fig. 6).

Similar CD spectra are obtained when LiOH is used instead of KOH to prepare a GBLi solution (Fig. S4†), again indicating that K^+ ions do not template detectable G-quartets under these conditions. Remarkably, the CD spectra on this GBLi sample confirm that it really is the dye, ***E*-1**, and not K^+ that induces formation and subsequent stacking of G-quartets. In another control experiment that underscores the importance of dye-templated formation of G-quartets, we found that solutions of KOH, boric acid and inosine, which cannot self-organize to give H-bonded macrocycles, show no optical activity in the presence of ***E*-1** (Fig. S5†). These above experiments confirmed that the G4 motif is essential for GBK/***E*-1** complexation. In addition, no CD signals are observed after addition of ***E*-1** to a GBK mixture prepared starting from 8-bromoguanosine (8-BrG) instead of guanosine. Since it is well known that 8-BrG favors a predominant *syn* conformation about its C1′–N glycosidic bond,[9] this lack of a CD signal indicating any chiral self-assembly of 8-BrG points to a strict stereochemical requirement for an *anti* conformation (as observed in NMR spectra for the GBK solution made from guanosine) in order for the GBK/***E*-1** supramolecular assembly to form.

Variable temperature CD experiments reveal that all CD band intensities increase upon cooling, while a strong hypochromic effect can be seen in the UV spectra (Fig. S6†), indicating an enhancement of π–π interactions for both the G4 layers and the dye's azo group at low temperature. Consistent with the NMR data shown above, CD spectroscopy also shows that the GBK/***E*-1** complex can be easily and reversibly destroyed by either heating (Fig. S6†) or by irradiating a r.t. sample with UV light (Fig. 6 and Fig. S4†). By irradiating the sample at 365 nm for 10 min the *cis*-photostationary state (PSS-*cis*) (see Experimental) is attained and all CD signals weaken, indicating an almost complete disaggregation of the GBK/***E*-1** complex to give monomeric Gs and ***Z*-1** dye. Subsequent irradiation (10 min) of the sample at 436 nm gives the *trans*-photostationary state (PSS-*trans*), where *ca.* 80% of the initial aggregation is recovered, as deduced from signal intensities. This photochemical cycle, which toggles the system between the assembled and disassembled states, can be repeated several times without significant fatigue either in the presence of K^+ or Li^+ (Fig. 7).

Results obtained from CD titration experiments (Fig. S7†) parallel the data presented previously from NMR titrations. As determined from CD signal intensities plotted against concentration of dye ***E*-1**, the amount of the GBK/***E*-1** complex increases linearly with added dye until the [total-G]/[***E*-1**] ratio in solution is ≥6, while further additions of dye produces progressively less aggregate.

Hence, all the combined NMR and CD spectroscopic data point to the essential role of the cyclic borate diester **GBG-1** in the self-assembly process. Indeed, no optical activity related to either stacked G4 units or exciton CD in the dye's absorption region are detected when ***E*-1** is added to either native guanosine or 2′-deoxyguanosine (treated under the same conditions used for GBK preparation) or a **GB** solution (obtained by reacting G with an excess of KOH and boric acid), which does not contain GBG diesters (Fig. S5†). This last observation also rules out the existence of fast equilibria among the various G species in solution, which might be shifted towards formation of **GBG-1** upon addition of dye ***E*-1**: thus, the composition of the initial GBK mixture is not altered by addition of ***E*-1**.

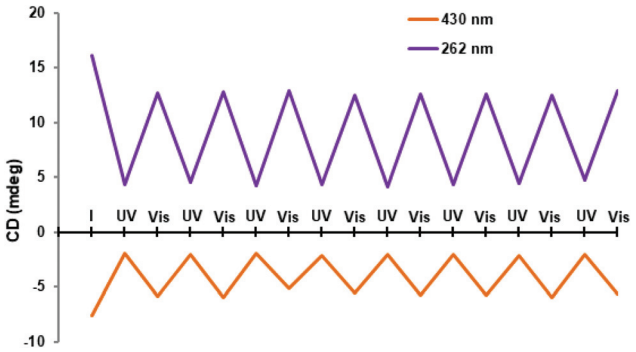

Fig. 7 Plot of the photoinduced variation of CD values (ellipticity) measured on a 3 : 1 10 mM GBK/**1** solution at 262 and 430 nm, upon irradiation with 365 and 436 nm light (irradiation time 10 min for each step). I, UV, and Vis refer to the initial, 365 nm photostationary, and 436 nm photostationary states, respectively. Eight subsequent irradiation cycles are shown.

X-ray scattering

SAXS experiments are performed as a function of GBK (as total G) concentration (ranging from 10 mM to 30 mM, *i.e.* from solution to gel state) and in the presence of different amounts of ***E*-1**. SAXS curves are reported in Fig. 8 and clearly indicate that aggregation occurs in all the investigated cases. Besides the 10 mM GBK solution in the absence of dye (gray trace in Fig. 8), which will be discussed below, at least three different SAXS characteristic profile patterns can be identified, confirming the occurrence of a complex supramolecular polymorphism. The first pattern is observed for the more dilute solutions (10 mM) and at low ***E*-1** content ([GBK]/[***E*-1**] ≥ 16), *i.e.* in the *sol* phase and in the presence of an amount of dye insufficient for complete complexation. This profile (type *a*, blue in Fig. 8) is characterized by a low and noisy SAXS intensity, which in a log–log representation shows a continuous decay as a function of Q.

The second pattern (type *b*, green in Fig. 8) characterizes samples prepared at 10 mM GBK (*sol*) and 20 mM GBK (*gel*) with relatively high amounts of ***E*-1** (molar ratio = 4, *i.e.* in the presence of an excess of dye with respect to the amount required for complete G4 formation): an extended Guinier region, which corresponds to a flat low-Q behavior in the log–log plot, is indeed observed. The third pattern (type *c*, red in Fig. 8) is detected for samples prepared at GBK concentrations ≥20 mM (*i.e.*, above the critical gelation concentration of 15 mM) and with a low or null ***E*-1** content: here the scattering

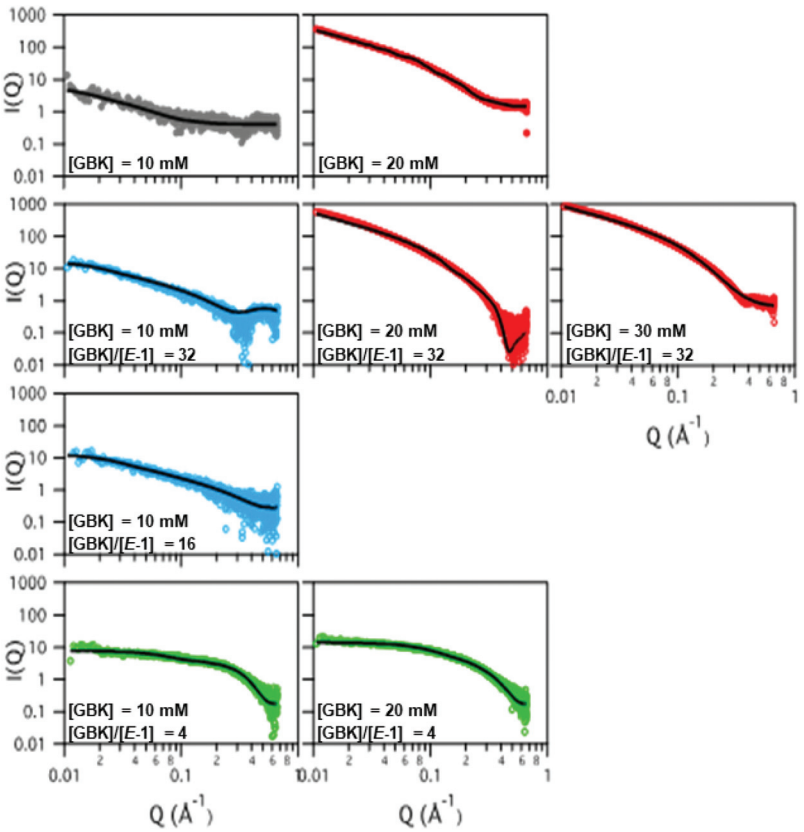

Fig. 8 log–log plots of SAXS data at 25 °C for different GBK/***E*-1** mixtures. Colors refer to the different observed patterns (see text). Lines are fittings to the experimental data.

is strong and distinctive of the presence of a partially ordered system. This *c* profile is compatible with the formation of the gel phase, as already detected by Peters *et al.* under analogous experimental conditions by visual inspection of samples and by vial inversion experiments.[7] In particular, as observed for hydrogels based on G4,[10] a *fan-like* scattering is detected for almost all the investigated GBK gel samples, suggesting the presence of an oriented network, which remains oriented for a quite large range of temperatures (see SAXS results for the 20 mM GBK sample in the absence of dye, reported in Fig. S8†).

In order to extract structural information, the SAXS curves are fitted by using a simple model for quadruplexes: straight cylinders with length L and cross-section of radius R. According to the G4 structure, the cross-sectional electron density profile of the cylinder has been split into two homogeneous regions: an inner region, of radius R_{core} and electron density ρ_{core}, where guanine residues are expected to be located, and a shell of thickness $t_{shell} = (R - R_{core})$ and electron density ρ_{shell}, which corresponds to the aqueous sugar and boron region.[11] Fitting results are shown as black traces in plots of Fig. 8, while a few fitted parameters are reported in Table 1. Interestingly, the core–shell cylinder model is very appropriate to reproduce the SAXS curves obtained in all the investigated conditions, with the exception of the curve corresponding to the sample at low GBK concentration (10 mM) and absence of dye. In this case, a ribbon model is applied instead to best fit the SAXS curve.[11]

Model parameters in Table 1 confirm that the different profiles correspond to different aggregation states. In the case of 10 mM GBK and absence of ***E*-1** (gray profile in Fig. 8), planar, tape-like H-bonded guanine ribbons form, with a structure probably similar to the ones described for lipophilic guanosines in aprotic solvents.[8] At this low GBK concentration, addition of ***E*-1** induces the appearance of cylindrical aggregates. Up to a [GBK]/[***E*-1**] molar ratio = 16, comparison of the fitted cross-section dimensions with models (Table S1†) indicates that G-quadruplexes made by **GBG-1** probably form (**Q1** in Fig. 1). When the amount of dye increases (molar ratio = 4), the cross-section dimensions suggest that all the four molecular G analogues ($\mathbf{G_{unr}}$, **GB**, **GBG-1** and **GBG-2**) are involved in the G-quadruplex structures (**Q2** in Fig. 1). Indeed, the whole radius for molar ratios of 32 and 16 is about 10 Å, while it increases to about 15 Å when [GBK]/[***E*-1**] becomes 4. Note that cylinders become shorter as the amount of ***E*-1** increases: according to titration data, the dye-mediated stacking forces probably reduce (or are less effective in stabilizing the aggregate) when the different G species are participating in complex formation. Thermal stability is however high, as indicated by SAXS results obtained on heating (see Fig. S8†): model fitting

Table 1 Geometrical parameters of the core–shell cylinder model used to best fit the SAXS curves: R_{core}, R and L are the radius of the core region and the external radius and length of the cylinder, respectively. For 20 and 30 mM samples, the symbol ∞ indicates that the length of the cylinder is too big to be determined. For the dye-free 10 mM GBK, a ribbon model with elliptical cross-section has been considered: its parameters are indicated with * and correspond to the minor and major semi-axes of the ellipsis. k is a normalization constant. Cell colors reflect the different profiles (see text) according to Fig. 8. Errors in parameter values are estimated to be in the 10 to 15% range

	GBK concentration (mM)														
	10					20					30				
[GBK]/[***E*-1**]	Profile	R_{core} (Å)	R (Å)	L (Å)	k (10^{-10})	Profile	R_{core} (Å)	R (Å)	L (Å)	k (10^{-10})	Profile	R_{core} (Å)	R (Å)	L (Å)	k (10^{-10})
No dye		3.1*	11.6*	290	0.65	*c*	6.5	18.7	∞	0.62	—	—	—	—	—
32	*a*	6.0	9.6	220	4.8	*c*	8.1	24.8	∞	1.2	*c*	9.8	30.7	∞	1.5
16	*a*	6.5	10.0	180	6.4	—	—	—	—	—	—	—	—	—	—
4	*b*	6.0	15.3	62	7.9	*b*	6	15.0	65	8.4	—	—	—	—	—

indicates that R_{core} and R are almost constant (6.0 ± 0.9 and 8.9 ± 0.9 Å, respectively), while the quadruplex length L slightly reduces from 62 ± 3 to 53 ± 5 Å on moving from 5 to 80 °C. At higher GBK concentrations, the SAXS data show that the properties of the aggregates are different. At absent or low dye content, very long cylindrical aggregates form: their cross-section dimensions are compatible with formation of long G-quadruplexes made from all the four G species. Under these conditions the stable G-quadruplexes are sufficiently flexible to create a 3D network able to entrap a large amount of water and to lead to formation of a self-standing and self-supporting hydrogel.[7,10]

Increasing the amount of dye up to a molar ratio [GBK]/[***E*-1**] = 4 results in the disruption of the gel phase and in the formation of shorter G-quadruplexes, whose cross-section dimensions still suggest the involvement of all the different molecular G species in the aggregation process. However, the structures of the G-quadruplexes in the two cases are different, as evidenced by high-angle X-ray scattering experiments performed on the 20 mM samples. Fig. 9 shows in the absence of dye, or for [GBK]/[***E*-1**] = 32, the presence of a diffraction peak at Q = 18.5 nm^{-1}, indicative of a regular stacking of self-assembled G4 with a stacking distance of 3.4 Å.[11] The peak at Q = 18.5 nm^{-1} is no longer present in the sample with [GBK]/[***E*-1**] = 4, indicating that the G4 are no longer π-stacked, and G-quadruplex formation is possibly templated by intercalation of the dye (**Q2** in Fig. 1).

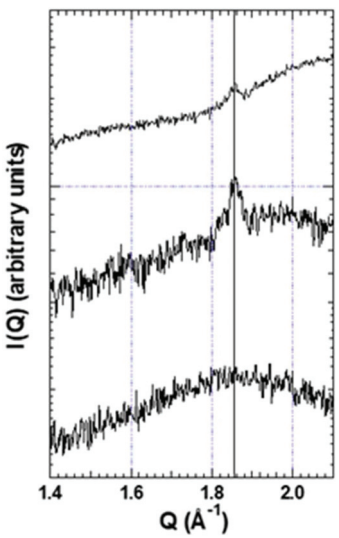

Fig. 9 High-angle X-ray diffraction results for the 20 mM GBK samples. From top: no ***E*-1**, [GBK]/[***E*-1**] = 32 and [GBK]/[***E*-1**] = 4, respectively. The vertical line is a guide to the eye to follow the peak position.

Discussion

Inspection of models (Fig. 10) reveals that the two diastereomeric borate diesters, whose assignment of ^{1}H NMR signals has so far not been possible, have markedly different shapes. One diester (**GBG-2**) has a "stretched W" shape, with the two guanines almost coplanar but pointing in opposite directions. The other diester (**GBG-1**) has a "C" shape, with the two nucleobases in a sort of eclipsed configuration, due to the rigidity of the borate linkage. Given the *anti* conformation around the glycosidic bond observed by NMR, the two guanines in **GBG-1** are facing each other in a tail-to-tail arrangement and form a dihedral angle of about 20 degrees (as measured between the two C1′–N glycosidic bonds). The two nucleobases are at a distance of *ca.* 5.3 Å, leaving just enough room to accommodate and π-stack with a flat guest molecule such as ***E*-1**. In other words, the diester **GBG-1** has a pocket where the ***E*-1** dye can bind using both π–π stacking and ionic interactions.

We propose that a transient host–guest complex between **GBG-1** and ***E*-1** (**IC** in Fig. 1) is the germination species, which, in a domino fashion, templates the simultaneous formation of two adjacent but not π-stacked G-quartets (an octamer, **Oc** in Fig. 1), where both host and guest attain further stabilization. Octamers formed in this manner immediately pile up into larger G-quadruplexes (**Q1** in Fig. 1), involving further intercalation of more dye. For low dye concentrations, SAXS and NMR data point to a selective involvement of **GBG-1**: data suggest that these first G-quadruplexes (**Q1**) involve mainly – if not only – this diester. It must be pointed out that we have no direct spectral evidence for both the host–guest complex (**IC** in

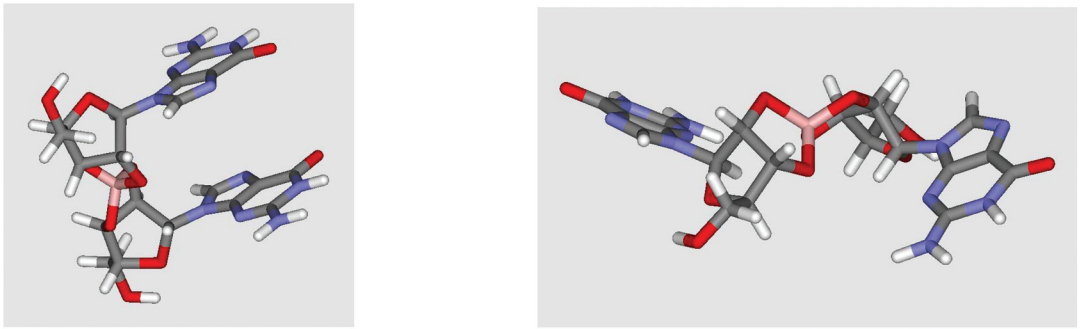

Fig. 10 Molecular models of the diastereomeric borate esters, **GBG-1** (left) and **GBG-2** (right). The diester **GBG-1**, unlike **GBG-2**, has a cleft that favors binding of the dye ***E*-1** by the two adjacent guanine bases.

Fig. 1) and the octamer (**Oc** in Fig. 1) as stable, isolated species. Sintim demonstrated that an octameric species analogous to **Oc** is involved in c-di-GMP quadruplex formation mediated by thiazole orange.[12] ESI-MS analysis of GBK mixtures containing small amounts of ***E*-1** (1 : 32–1 : 16 ***E*-1** to G ratios) does not show the **IC** signal, while a weak cluster centered at *m*/*z* 1379.5 ($\mathbf{Oc}^{2-}$) can be observed, but clusters of analogous abundance attributable to other mixed octameric aggregates are also present in the spectra. Nonetheless, this cartoon-like sequence of events explains the overall behavior observed. When the amount of dye is increased, the other G species ($\mathbf{G_{unr}}$, **GB** and **GBG-2**) present in solution, which are far less effective in complexing the dye, become involved in G4s of the complex (**Q2** in Fig. 1) in a statistical way. Isomerization of the dye to the *Z* form involves bending of the guest, and this leads to dissociation of the host–guest complex and consequent disruption of the G-quartets, which in turn triggers collapse of the supramolecular G-quadruplex.

Unfortunately, attempts to separate the two diastereomeric borate diesters **GBG-1** and **GBG-2** either by crystallization or by reverse phase HPLC, as well as attempts to shift the 1 : 1 diastereomeric ratio during GBK/dye mixture preparation, *e.g.* by preparing the GBK mixture in the presence of dye at different temperatures or by thermally "post-curing" the GBK/dye mixture, have been unsuccessful so far.

At the low guanosine concentrations (5–15 mM) that we are working with, there is no "pre-folded" G-quartet detectable in solution by either ^{1}H NMR or CD. Thus, we cannot measure the affinity of either ***E*-1** or ***Z*-1** for G-quartets made from this GBK mixture. In fact, it is the ***E*-1** compound that templates formation of G-quartet. In earlier work Wang *et al.*[3a] did measure affinities of ***E*-1** and ***Z*-1** for a pre-folded DNA G-quadruplex. They found a value of 3.9×10^6 M^{-1} for the ***E*-1** binding to telomere DNA ($d(TTAGGG)_4$) while ***Z*-1** did not bind to G-quadruplex DNA, and we believe our data show the same trend for GBK binding to the dye **1**. Addition of ***E*-1** leads to formation of G-quartets, photochemical irradiation to give ***Z*-1** leads to complete loss of any G4 (NMR and CD).

In previous studies on GBG hydrogels,[7c] where we were working with higher concentrations of GBK (typically 50–100 mM), we have observed that known G4-ligands such as the cationic dyes crystal violet, thiazole orange and methylene blue facilitate G4-polymerization. However, we have never observed, until now, a small molecule templating G-quartet formation in water solution at such low concentration (10 mM). In addition, the disappearance of G4 supramolecular structures upon photoisomerization clearly suggests that ***Z*-1** has no such ability to template G4-assembly.

The CD spectrum of the ***E*-1**/GBK system shows a striking similarity with the one reported by Zhou[6] for the human telomeric sequence $d(TTAGGG)_4$ in the presence of similar dyes. In this latter case, the spectrum was interpreted in terms of a parallel G quadruplex structure. In our case the interpretation of the excitonic signals in the nucleobase region is not so straightforward, as this system composed of G nucleosides is different in many aspects from the one formed using G-rich DNA. The templating host–guest complex between **GBG-1** and ***E*-1** also controls the stereochemistry of the supramolecular assembly: the *anti* conformation in diester **GBG-1** drives formation of the "octameric" intermediate towards a heteropolar tail-to-tail arrangement, with the two G4s held apart by the rigid borate-sugar backbone and twisted by an unusually small twist angle (<5° according to models).[13] The subsequent piling-up of octamers can thus only occur *via* head-to-head heteropolar stacking, with no further backbone constraints. In addition, in our case G4s are never stacking directly, but the stacking seems mediated by a dye molecule. In the DNA case, heteropolar stacking usually results in a positive CD signal at 290 nm and a negative couplet centered at 250 nm, as CD spectra of G-quadruplexes have shapes dominated by the stacking polarities of adjacent G4s.[14] When only non-covalent interactions exist between adjacent G4, as in the case of lipophilic guanosine derivatives, it is known that the effect of stacking polarities can be apparently reversed in simpler cases (two stacked G4s), while no clear correlation between stacking polarities and CD shape seems to exist for more complex structures involving lipophilic Gs.[14] Accordingly, also in the present case, the shape of the CD spectrum seems mainly due to the specific rotation angle between neighboring G4s rather than to their stacking polarity.

Conclusions

Photocontrol over self-assembled systems is an actively pursued subject. In particular, G-quadruplex formation induced by a photocontrollable template may offer interesting possibilities in different fields. In this paper, we explored the possibility to obtain a photo-responsive hydrogel by adding a photoisomerisable cationic dye to a G4-based gel system. We found that the cationic dye ***E*-1** destabilized the G4-based hydrogel when relatively high concentrations (50–100 mM) of total G species were present. However, at low concentrations of total G (15 mM) the photoswitchable dye **1** had a remarkable impact on templating G4-based assemblies in solution. As described above, cationic dye ***E*-1** was even more effective than K^+ in templating formation of the G4-based supramolecular assembly. According to our data, at low *G* concentration (*i.e.* in solution, where GBK system does not spontaneously form G-quadruplexes) a cascade of constructive recognition processes operate in sequence: one specific component of the GBK mixture (**GBG-1**) complexes the dye and this, in turn, enables self-recognition of this specific component to form G4s. A subsequent recognition process involving other G species present in solution occurs mainly, if not only, upon increasing the amount of dye, to form relatively small dye-intercalated G-quadruplexes. These aggregates can be photoreversibly destroyed and reformed. In the case of a preformed gel (*i.e.* when *G* concentration is higher and G4 formation is spontaneous), addition of dye has a destabilizing effect likely due to dye intercalation, which overcomes piling up of G4 layers, and preferential sequestering of a specific component of the mixture. This results in fragmentation of the large stacked G-quadruplexes into shorter dye-intercalated aggregates and produces a macroscopic weakening of the gel matrix, which turns into a sol. From a slightly different perspective, it is interesting to notice that the ***E*-1** template we used, so effective in promoting the formation of G4-based suprastructures in solution, turns out to destabilize other, G4-based structures in the gel state. Attempts are still in progress to obtain pure **GBG-1** or its analogues, with the ultimate goal of studying the supramolecular cages that we propose are formed upon complexation of a templating molecule (see **Oc** in Fig. 1).

In this work we demonstrated, on a *quasi*-natural system composed of low molecular weight compounds, how a single self-assembly process can trigger a photoreversible cascade of supramolecular events in a domino fashion, where each event is a prerequisite for the subsequent one. This leads ultimately to a photocontrolled amplification of the degree of self-assembly.

Experimental

Materials and methods

Chemicals are purchased from Fluka and Sigma-Aldrich, and used without further purification. Derivative **1** is synthesized as reported by Zhou.[6] All NMR experiments are performed on a Varian Inova (600 MHz) instrument equipped with either a direct or a reverse probe. Circular dichroism measurements are carried out on a JASCO J-710 spectropolarimeter by using a circular quartz cell of 0.01 cm path length. When not otherwise specified, spectra are recorded at room temperature with a scanning speed of 100 nm min^{-1}, and ten consecutive scans are averaged for each sample. Variable temperature experiments are performed by using a Neslab RTE-111 circulator thermostat (temperature stability ± 0.5 °C).

Preparation of samples

Both the 10 mM aqueous solutions (GBK or GBLi) and the 20 or 30 mM GBK hydrogels are prepared by adding the appropriate amount of guanosine with 0,5 equivalents of $KB(OH)_4$ (or $LiB(OH)_4$) and following a procedure previously described.[7a] The same procedure is followed for inosine, 2′-deoxyguanosine and 8-bromoguanosine samples. The **GB** solution is obtained by reacting G with 4 eq. of KOH and boric acid. When desired, the fresh solutions or hydrogels are added with the selected amount of ***E*-1** (solid powder) and heated at *ca.* 100 °C to obtain a clear solution: in all cases, the absence of residual solid powders is carefully verified with the help of a magnifying lens. The samples are then left to rest at room temperature in the dark and analyzed after *ca.* 2 hours by CD or NMR. SAXS measurements are performed on samples after *ca.* 4 days.

X-ray scattering experiments

Small-angle X-ray scattering (SAXS) experiments are performed on the SAXS beamline at the Elettra Synchrotron (Trieste, Italy). The wavelength of the incident beam is λ = 1.54 Å and the explored *Q*-range extended from 0.01 to 0.6 $Å^{-1}$ (*Q* is the modulus of the scattering vector, defined by $4\pi \sin\theta/\lambda$, where 2θ is the scattering angle). Scattering data are recorded on a 2-dimensional detector and corrected for background, detector efficiency, buffer contributions and sample transmission. The 2D data are then radially averaged to derive $I(Q)$ *vs.* *Q* curves. G solutions are measured using 1 mm quartz capillaries at 25 °C. To avoid radiation damage, the exposure time is 300 s per frame.

A few high-angle X-ray diffraction (WAXS) experiments are also performed. A Philips PW1830 X-ray generator equipped with a Guinier-type focusing camera operating in vacuum and a bent quartz crystal (λ = 1.54 Å), is used. Diffraction patterns are recorded on GNR Analytical Instruments Imaging Plate system. Samples, held in a tight vacuum cylindrical cell provided with thin mylar windows, are analyzed at room temperature.

Photochemical isomerization

For experiments followed by CD/UV, photoisomerization is performed by irradiating the sample contained in a 0.01 cm quartz cell with the 150 W Xe lamp of the dichrograph. The monochromator of the instrument (slit width = 3 mm) is employed to select the irradiation wavelengths. The photostationary states are reached within 10 min by irradiating either

at 365 nm (PSS-*cis*) or 436 nm (PSS-*trans*), as deduced by monitoring the detector photocurrent decrease (at 365 nm) or increase (at 432 nm) till a constant value is obtained. For experiments followed by NMR, photoisomerization is performed by irradiating the sample contained in a standard NMR tube with a 150 W high pressure Hg/Xe lamp. Interference filters (Oriel) are used for selecting the irradiation wavelengths. The photostationary states are reached in 5 hours *ca.*, as evidenced by monitoring spectral changes.

Conflicts of interest

Q4 ■■■■

Acknowledgements

Financial support from University of Bologna (RFO) is gratefully acknowledged. M. C. thanks the Dept. "Giacomo Ciamician" for a Marco Polo grant. J. T. D. thanks the Office of Basic Energy Sciences, U.S. Dept. of Energy (DEFG02-98ER14888) for support.

References

1 (*a*) S. Li, A. Hao, J. Shen, N. Shang and C. Wang, *Soft Matter*, 2018, **14**, 2112–2117; (*b*) T. Ohtake, *Mol. Syst. Des. Eng.*, 2018, **3**, 804–818.

2 (*a*) F. Ercole, T. P. Davis and R. A. Evans, *Polym. Chem.*, 2010, **1**, 37–54; (*b*) M. Yamada, M. Kondo, J. Mamiya, Y. Yu, M. Kinoshita, C. J. Barrett and T. Ikeda, *Angew. Chem., Int. Ed.*, 2008, **47**, 4986–4988; (*c*) Y. Chen, Z. Wang, Y. He, Y. J. Yoon, J. Jung, G. Zhang and Z. Lin, *Proc. Natl. Acad. Sci. U. S. A.*, 2018, **115**, E1391–E1400; (*d*) J. Chen, F. King-Chi Leung, M. C. A. Stuart, T. Kajitani, T. Fukushima, E. van der Giessen and B. L. Feringa, *Nat. Chem.*, 2018, **10**, 132–138.

3 (*a*) S. Wang, L. Yue, Z.-Y. Li, J. Zhang, H. Tian and I. Willner, *Angew. Chem., Int. Ed.*, 2018, **57**, 8105–8109; (*b*) V. Adam, D. K. Prusty, M. Centola, M. Škugor, J. S. Hannam, J. Valero, B. Klöckner and M. Famulok, *Chem. – Eur. J.*, 2018, **24**, 1062–1066; (*c*) J. J. Keya, R. Suzuki, A. Md. R. Kabir, D. Inoue, H. Asanuma, K. Sada, H. Hess, A. Kuzuya and A. Kakugo, *Nat. Commun.*, 2018, **9**(453), 1–8.

4 (*a*) M. P. O'Hagan, J.-L. Mergny and Z. A. E. Waller, *Biochimie*, 2018, **147**, 170–180; (*b*) *Guanine quartets: structure and application*, ed. W. Fritzsche and L. Spindler, RSC, London UK, 2013.

5 (*a*) S. Ogasawara and M. Maeda, *Angew. Chem., Int. Ed.*, 2009, **48**, 6671–6674; (*b*) S. Lena, P. Neviani, S. Masiero, S. Pieraccini and G. P. Spada, *Angew. Chem., Int. Ed.*, 2010, **49**, 3657–3660; (*c*) J. Thevarpadam, I. Bessi, O. Binas, D. P. N. Gonçalves, C. Slavov, H. R. A. Jonker, C. Richter, J. Wachtveitl, H. Schwalbe and A. Heckel, *Angew. Chem., Int. Ed.*, 2016, **55**, 2738–2742.

6 (*a*) X. Wang, J. Huang, Y. Zhou, S. Yan, X. Weng, X. Wu, M. Deng and X. Zhou, *Angew. Chem., Int. Ed.*, 2010, **49**, 5305–5309; (*b*) X. Xing, X. Wang, L. Xu, Y. Tai, L. Dai, X. Zheng, W. Mao, X. Xu and X. Zhou, *Org. Biomol. Chem.*, 2011, **9**, 6639–6645.

7 (*a*) G. M. Peters, L. P. Skala, T. N. Plank, B. J. Hyman, G. N. M. Reddy, A. Marsh, S. P. Brown, S. R. Raghavan and J. T. Davis, *J. Am. Chem. Soc.*, 2014, **136**, 12596–12599; (*b*) G. M. Peters, L. P. Skala, T. N. Plank, H. Oh, G. N. M. Reddy, A. Marsh, S. P. Brown, S. R. Raghavan and J. T. Davis, *J. Am. Chem. Soc.*, 2015, **137**, 5819–5827; (*c*) G. M. Peters, L. P. Skala and J. T. Davis, *J. Am. Chem. Soc.*, 2016, **138**, 134–139.

8 (*a*) A. Ciesielski, M. El Garah, S. Masiero and P. Samorì, *Small*, 2016, **12**, 83–95; (*b*) G. N. M. Reddy, A. Huqi, D. Iuga, S. Sakurai, A. Marsh, J. T. Davis, S. Masiero and S. P. Brown, *Chem. – Eur. J.*, 2017, **23**, 2315–2322.

9 (*a*) W. Saenger, *Principles of Nucleic Acid Structure*, Springer-Verlag, New York, 1984; (*b*) E. Dias, J. L. Battiste; and J. R. Williamson, *J. Am. Chem. Soc.*, 1994, **116**, 4479–4480.

10 F. Carducci, J. S. Yoneda, R. Itri and P. Mariani, *Soft Matter*, 2018, **14**, 2938–2948.

11 (*a*) A. Gonnelli, M. G. Ortore, E. J. Baldassarri, G. P. Spada, S. Pieraccini, R. C. Perone, S. S. Funari and P. Mariani, *J. Phys. Chem. B*, 2013, **117**, 1095–1103; (*b*) P. Mariani, F. Spinozzi, F. Federiconi, H. Amenitsch, L. Spindler and I. Drevensek-Olenik, *J. Phys. Chem. B*, 2009, **113**, 7934–7944.

12 S. Nakayama, I. Kelsey, J. Wang, K. Roelofs, B. Stefane, Y. Luo, V. T. Lee and H. O. Sintim, *J. Am. Chem. Soc.*, 2011, **133**, 4856–4864; S. Nakayama, I. Kelsey, J. Wang and H. O. Sintim, *Chem. Commun.*, 2011, **47**, 4766–4768.

13 R. V. Reshetnikov, A. M. Kopylov and A. V. Golovin, *Acta Naturae*, 2010, **2**, 72–81.

14 S. Masiero, R. Trotta, S. Pieraccini, S. De Tito, R. Perone, A. Randazzo and G. P. Spada, *Org. Biomol. Chem.*, 2010, **8**, 2683–2692.